연 구 논 문

SS400-STS304 이재용접부의 외력작용시 용접잔류응력 특성

방희선[*] · 방한서[*] · 김유철[**] · 주성민[***] · 좌순원[****] · 노찬승[*****,†]

[*]조선대학교 공과대학 선박해양공학과
[**]일본 오사카대학교 접합과학연구소
[***]포항산업과학연구원 용접센터
[****]경남도립거창대학 조선공학과
[*****]조선이공대학 선박해양·기계공학과

Influence of Welding Residual Stress on the Mechanical Behavior of Externally Loaded Dissimilar SS400-STS304 Steel Weldment

Hee-Seon Bang*, Han-Sur Bang*, You-Chul Kim**, Sung Min Joo***,
Soon-Won Joa**** and Chan-Seoung Ro*****,†

*Dept. of Naval Architecture & Ocean Engineering, Chosun University, Gwangju 501-759, Korea
**Joining & Welding Research Institute, Osaka University, Osaka 567-0047, Japan
***Welding Center, Research Institue of Industrial Science and Technology, Pohang 790-330, Korea
****Dept. of Naval Architecture Engineering, Gyeongnam Provincial Geochang College, Geochang 670-804, Korea
*****Dept. of Naval Architecture & Mechanics Engineering, Chosun College of Science and Technology, Gwangju 501-744, Korea

†Corresponding author : csro@chosun-c.ac.kr

(Received November 10, 2008 ; Revised January 14, 2009 ; Accepted September 24, 2009)

Abstract

Thermal and mechanical characteristics in dissimilar SS400-STS304 steel weldment have been investigated by 3D thermal elastic-plastic analysis. Moreover, the influence of welding residual stresses on the mechanical behaviour of this welded joint, by applying superimposed external load (tension load) was determined. The residual stresses obtained by numerical simulation were compared with the experimentally measured results. The FE results were in good agreement with the measured values. The mechanical test (hardness, tensile test) and metallurgical analysis was carried out to ensure the weld integrity. Hence, possibility of applying SS400-STS304 dissimilar steels in industries has been established.

Key Words : Dissimilar SS400-STS304 steel weldment, 3D thermal elastic-plastic analysis, Welding residual stress, External load

1. INTRODUCTION

Residual stresses and distortions are two of the major concerns in welded structures. Welding residual stresses not only cause distortion but also significantly affect the service characteristics of welded structures. The residual stresses in weld region are normally tensile and close to the material yield stress due to the shrinkage of the weld on cooling. The combination of high tensile residual stresses in weld region and tensile loads applied can promote brittle fracture that increases the susceptibility of weld to fatigue damage[1,2]. Notably, welding of dissimilar materials produces different residual stresses because of the differences in the coefficient of thermal expansion and heat conductivity of the two welded materials, compared to similar materials; knowing of residual stress level allows avoid the failure of welded joints.

In the present study, thermal conduction and thermal elasto-plastic numerical analysis was performed using a developed program[3] to clarify the welding residual stress and plastic strain characteristics of dissimilar SS400-STS304 steel weldment. In order to verify the numerical simulation results, welding residual stress results obtained by numerical analysis on dissimilar SS400-STS304 steel weldment were compared with the experimentally measured residual stresses results. The strength of this dissimilar welded joint was evaluated by mechanical test (hardness, tensile test) and metallurgical analysis. Moreover, longitudinal residual stresses, which are most harmful to the integrity of the structure among the residual stress components, have been investigated by applying superimposed external load (tension load).

2. RESEARCH METHODS

2.1 Numerical analysis

2.1.1 Theoretical background for heat transfer and thermal elasto-plastic FE analysis

When welding is carried out over a considerable length, heat flow attains a quasi stationary state that can be treated as a steady state flow problem for a moving coordinate in the whole welded area, except in areas near the start and end of welding. Therefore, in the present work the heat conduction and thermal elastic-plastic analysis is carried out in areas remote from end effects, assuming heat flow is in a quasi stationary state. For the formulation of finite elements of the thermal-elastic-plastic computer program, the governing equation of a non-stationary heat conduction problem when the material is isotropic and continuous is given by equation (1) as

$$\rho c \frac{\partial T}{\partial t} = \lambda \nabla^2 T = Q \tag{1}$$

where, T is temperature (℃), ρ is density ($g\text{-}cm^{-3}$), Q is rate of temperature change due to heat generation per volume ($cal\text{-}cm^{-3}.sec^{-1}$), t is time (sec), λ is thermal conductivity of isotropic material ($cal\text{-}cm^{-1}.sec^{-1}.℃^{-1}$) and c is specific heat ($cal\text{-}g^{-1}.℃^{-1}$)[4].

The temperature dependent material properties such as yield strength and elastic modulus are considered, through the elastic and plastic regions, for the welding residual stress and strain program. In the elasto-plastic problem, the total increment of strain is the summation of increment in elastic strains, plastic strains and thermal strains and is given by equation (2) as

$$\{d\varepsilon\} = \{d\varepsilon^e\} + \{d\varepsilon^p\} + \{d\varepsilon^T\} \tag{2}$$

where, $\{d\varepsilon^e\}$ increment of elastic strain, $\{d\varepsilon^p\}$ increment of plastic strain and $\{d\varepsilon^T\}$ increment of thermal expansion strain.

Data transferring between commercial FE package and developed PATRAN Command Language (PCL) program can be compiled directly from the PATRAN desktop which is used for making a basic interface between the developed in-house solver and commercial package ANSYS.

2.1.2 Method of numerical analysis

The principal dimension of the model for numerical analysis is shown in Fig. 1(a). It is assumed that a 400×400×15 mm size specimen model is sufficient for a good simulation of a real process. The materials properties of mild steel SS400 and stainless steel STS304, as per KS (Korean Standards) were considered. The chemical compositons of base metals and welding condition for dissimilar steel are given in Table 1 and 2 respectively. SS400-STS304 steel weldment with 15mm thickness is performed using five-

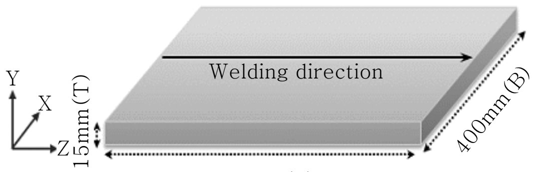

(a) Configuration of welded specimen and coordinate

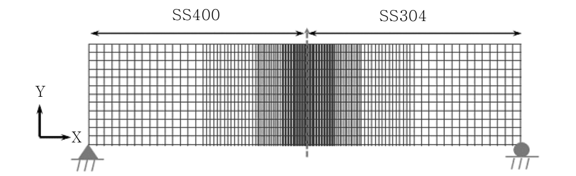

(b) FE model and boundary condition for numerical analysis

Fig. 1 Welded specimen details and boundary condition for analysis

pass welding process. The groove angle is selected as per the welding standards and similar groove dimension is considered for simulation also.

The MIG welding method is conducted with the STS 309 welding rod. Boundary condition for the elasto-plastic analysis was considered with actual restrained condition as shown in Fig. 1b. The mesh is made finer at the weld zone to get the accurate results. Physical and mechanical properties of mild steel (SS400) and STS304 is shown in Fig. 2 and 3[5].

Table 1 Chemical compositions of SS400 and STS304 steels (wt.%)

Material	C	Si	Mn	P	S	Ni	Cr	Mo
SS400	0.16	0.32	1.63	0.008	0.013	0.03	0.04	-
STS304	0.032	0.46	1.43	0.028	0.028	8.55	18.2	0.29

Table 2 Welding condition and process parameters

Model	Welding process	Current (A)	Voltage(V)	Speed (Cm/min)
SS400 - STS304	MIG	AC 110	20	25
Welding pass				

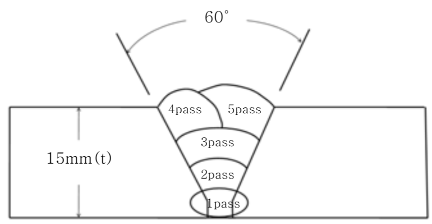

2.2 Experiment details

Specimen of 400×400×15 mm size was welded with MIG welding process. Welding residual stress is measured by sectioning techniques of stress-relaxation method (non-destructive method) using strain gauges near the weld region. The checkpoints for welding residual stresses were selected in accordance with the result of

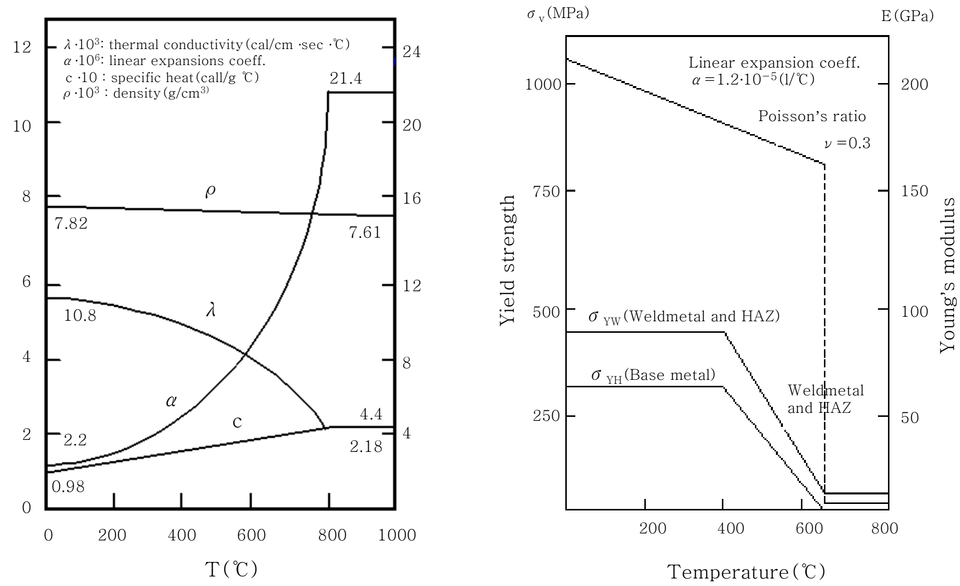

Fig. 2 Physical and mechanical properties of SS400

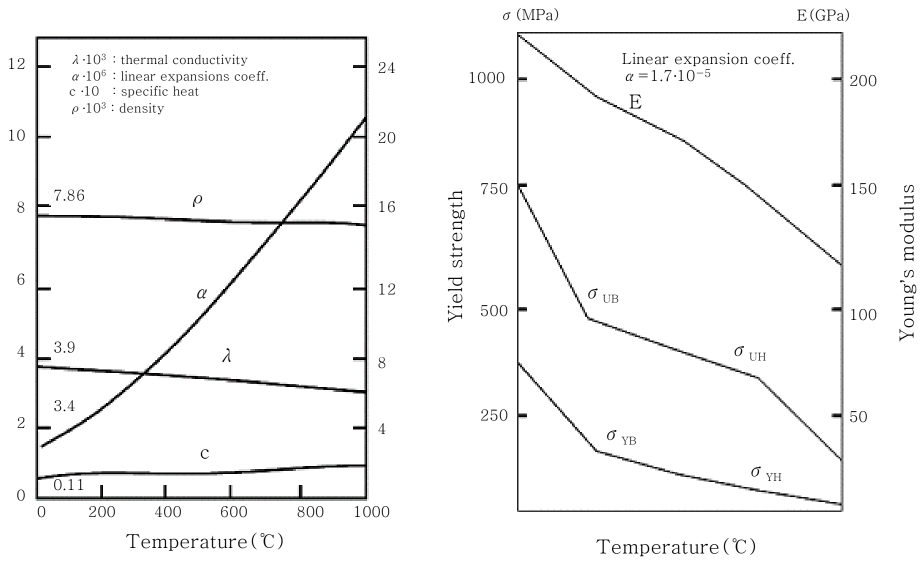

Fig. 3 Physical and mechanical properties of STS 304

numerical analysis and measurement is carried out at the centre (z = 200mm) along the width direction of weldment. Mechanical tests such as tensile test, hardness test and micro-structure analysis were carried out in order to establish the mechanical phenomenon of welded joint experimentally. Tensile test is carried out under a perpendicular load to the weld axis with a crosshead speed of 5mm/min. Vickers hardness is measured near weld metal with the load 10kgf. The hardness was measured at points, 2mm away from the upper part. An image analysis technique is utilized to determine the porosity fraction and the microstructure is observed by scanning electron microscopy (SEM).

3. RESULTS AND CONSIDERATIONS

3.1 Numerical Analysis results

3.1.1 Thermal characteristic of dissimilar steel weldment

By using the non-stationary thermal conduction program, the results obtained from the thermal characteristics analysis in welded joint were compared. The characteristics of thermal distribution, that cause residual stresses, have been investigated.

Fig. 4 illustrates the temperature field after

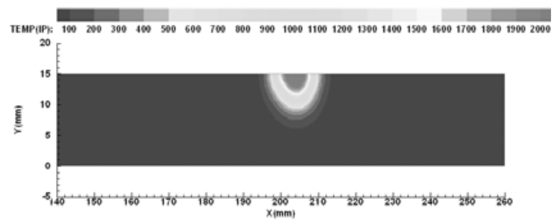

(a) Transient temperature distribution after 2 sec in heating stage

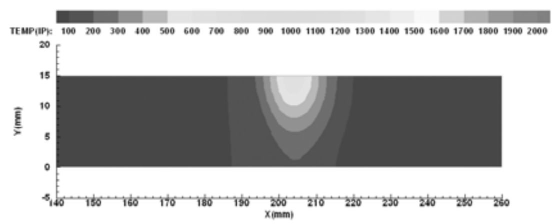

(b) Transient temperature distribution after 10.35 sec in cooling stage

Fig. 4 Temperature field after the 5th pass welding of the dissimilar steel weldment

heating the 5th weld pass in the welded joint. The heat dissipates into SS400 more rapidly than STS304, which means that the thermal conduction of SS400 is higher than that of STS304. Fig. 5 shows the temperature variation of elements, at 6mm depth from the upper surface of plates, along the direction of width of welded joint from sec 2 sec to 36 sec. The maximum heating and minimum cooling temperature appears in dissimilar steel weldment at 2

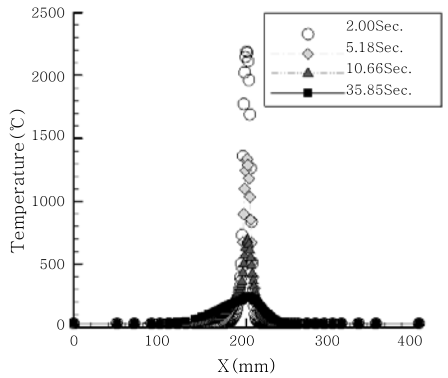

Fig. 5 Temperature variation of the dissimilar steel weldment

seconds and 35.85 seconds respectively, after the commencement of welding From the analysis results, it is found that the temperature changes abruptly in the vicinity of weld and gently as being away from the welds. Besides, temperature gradient appeared sluggishly with respect to time. When comparing SS400 and STS304 during cooling, it is showed that SS400 has the gently-slopping temperature gradient and the thermal conduction progresses faster in SS400.

3.1.2 Mechanical characteristic of dissimilar steel weldment

The developed thermal elasto-plastic program simulates the mechanical phenomenon of welding residual stress and plastic-strain in dissimilar joint weldments. Fig. 6 illustrates the welding residual stress and plastic strain, caused along the direction of thickness. When observing the characteristic of welding residual stress of each component, if weld metal is cooled down below 700℃, it recovers its mechanical rigidity and stress, which is generated in weld metal as its contraction is restricted by base metal in vicinity of weld during cooling[6]. In Fig. 6, residual stress in the longitudinal direction indicates the tension along the longitudinal direction σ_z of weld metal and heat affected zone, and reaches maximum in HAZ, and changes to compression in base metal in vicinity of HAZ. Especially, residual stresses σ_y in the thickness direction are higher and the minimum value appears on residual stress σ_x in the transverse direction. While comparing the magnitude of stress values, dissimilar steel weldment shows stresses in the order $\sigma_z \rangle \sigma_y \geq \sigma_x$. This indicates that weldment experiences the different amount of mechanical restraint. When comparing residual stress for base metal, residual stress σ_x in the transverse direction is higher in STS304 and residual stress σ_y in the thickness direction is higher in SS400 respectively. This implies that the mechanical restraint conditions are different in both materials after welding. The plastic strain ε_z^p in the longitudinal direction is in compression at HAZ and in tension at weld, the plastic strainε_x^pin the transverse direction and the plastic strain ε_y^p in the thickness direction is in tension at heat affected zone and in compression at weld metal. The magnitude of absolute value of plastic strain ε_z^p in the longitudinal welding direction is comparatively high. The characteristics, mentioned above, were considered that the tensile plastic strain occurs along the Z-axis where it is restrained most highly and the compressive plastic strain occurs along the X-axis and Y-axis where it is restrained slightly.

3.1.3 Mechanical characteristic of dissimilar steel weldment under superimposed external load

Fig. 7 shows the comparison of stress distribution in dissimilar steel weldment, with and without welding residual stress, under superimposed tension load. The residual stress is measured for different tension loads at mid section (y=7.5mm) of the specimen model. The tension loads from 1.6 to 4.8Ton are superimposed to edge of the weldment in order to observe the welding residual stress effect on external loading. The welding residual stress is used in ANSYS as initial stress and FE analysis is carried out by varying the tension load from 0Ton to 4.8Ton, the value that are obtained from experiment. The difference in residual stress distribution has been clearly noticed when comparing the obtained results as shown in Fig. 7(a) and Fig. 7(b). As shown in Fig. 7 (b), the residual stress of welded structure increases keeping shape of

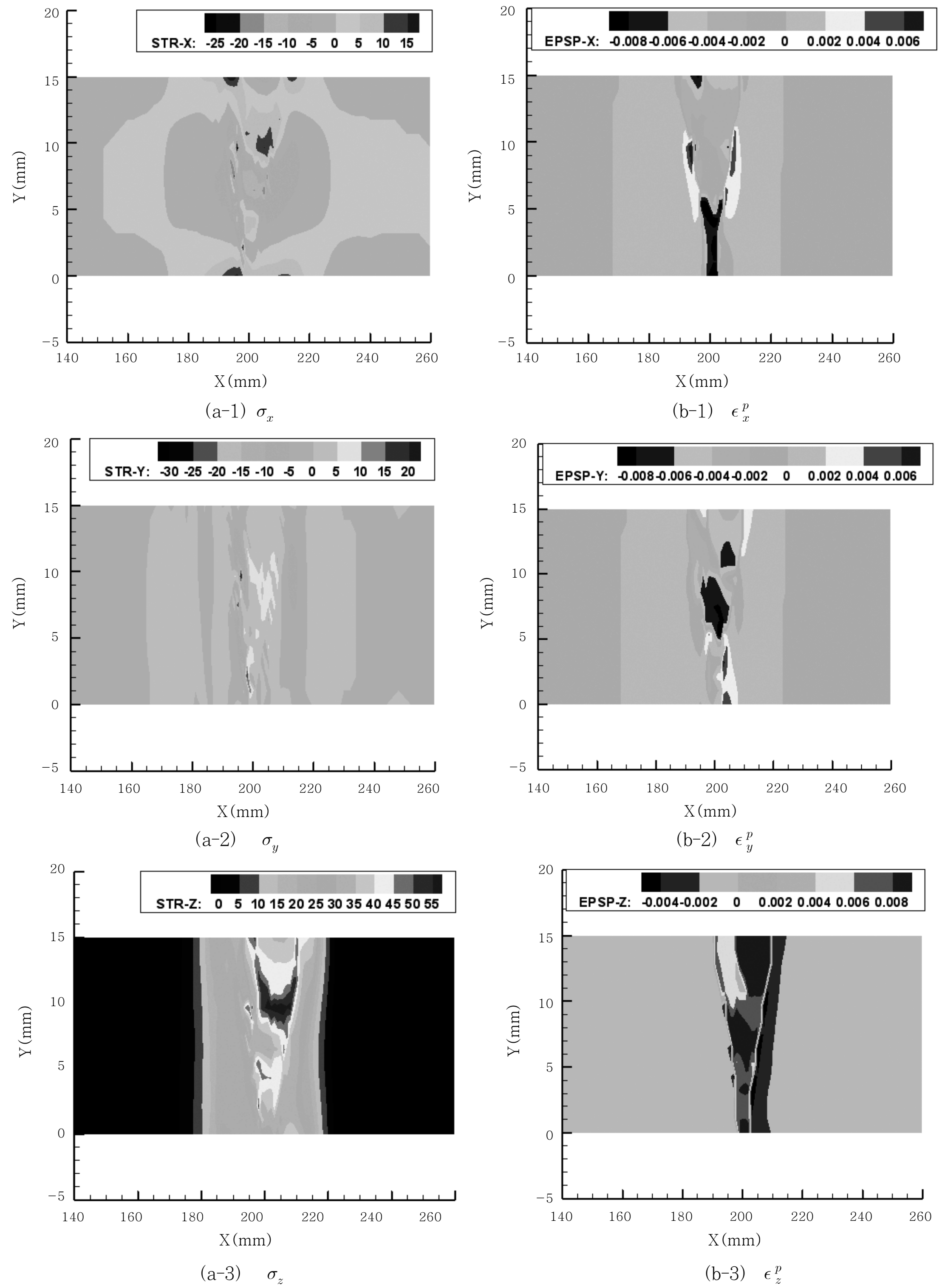

Fig. 6 Residual stress (a) and plastic strain (b) distribution of the dissimilar weld joints in X, Y and Z directions

pre-stress, as tension load increases. Starting from initial load, for each increment of 1.6Ton, residual stresses is found increasing by 14% and redistributes. From the results, it is revealed when tension loads are superimposed to the weldments, the longitudinal tensile stress σ_z in weld metal and heat affected zone, is increased significantly to a higher value.

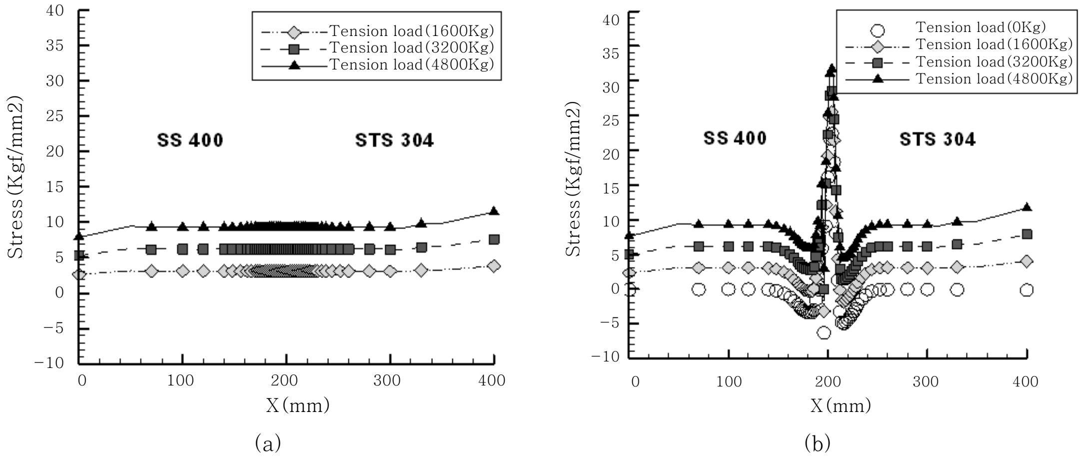

Fig. 7 Comparison of stress distribution in dissimilar steel weldment without and with residual stress under superimposed tension load measured at 7.5mm below top surface (a) without (b) with welding residual stress

3.2 Experimental results

Residual stress results by measurement at top surface were compared with numerical simulation at 1mm below top surface. When comparing the numerical simulation results and the measured values, it is found that same pattern of residual stresses distribution has been observed and the measured values are slightly lower than numerical results as shown in Fig. 8.

Table 3 shows the strength characteristics of dissimilar steel weldment that is obtained by tensile test. The fracture is generated at base metal, SS400, slightly away from HAZ in all specimens. The strength appears higher than that of SS400. It is revealed that tensile strength is about 53.4 Kgf-mm^{-2} and the range of tensile strength was scattered from 53.4 to 57.2 Kgf-mm^{-2}.

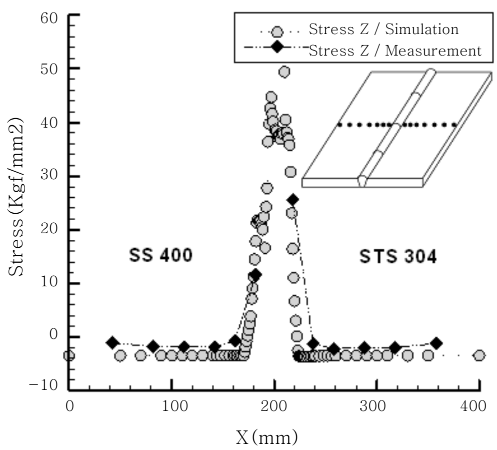

Fig. 8 Comparison of residual stress results by measurement at top surface and numerical simulation at 1mm below top surface

Table 3 Tensile properties of dissimilar SS400-STS304 steel welding specimens

Specimen no.	Yield strength (Kgf-mm^{-2})	Tensile strength (Kgf-mm^{-2})	Ductility rate (%)
1	36.3	53.7	28.3
2	40	53.4	30.8
3	35.3	57.2	29.5
4	36.3	53.7	29.3
5	35.6	53.6	30.5

Fig. 9 shows the hardness distribution of dissimilar SS400-STS304 steel weldment. The base metal, HAZ and weld metal of dissimilar steel weldment have similar magnitude of hardness in STS304 and the values were found decreased in SS400. Hardness reached the maximum value at weld metal because of the effect of dendrite. The micro-structures for weld metal, HAZ and base metal are pictured and examined to figure out the change of micro-structure characteristics in dissimilar steel weldment.

As shown in Table 4, base metal of STS304 of dissimilar welding specimen consists of austenite crystal grain and ferrite band, and it is seen that crystal grains are coarsened and carbide is

Table 4 Micro structural variation in different locations of dissimilar steel weldment

Specimen	W.M	HAZ	B.M
STS 304	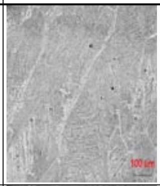	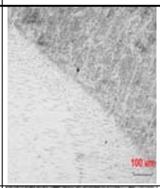	
SS 400	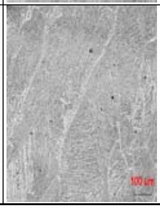	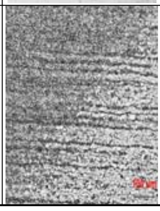	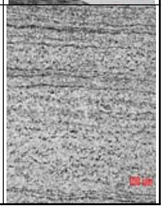

educe in vicinity of HAZ, and dendrite are formed in weld metal because it cools down rapidly after welding. It can be confirmed that the welding condition of dissimilar SS400-STS304 steel weldment seems good from the obtained sound results through mechanical and metallurgical characteristics evaluation.

CONCLUSION

1) The magnitudes of each components of residual stress shows the order $\sigma_z > \sigma_x \geq \sigma_y$ for dissimilar steel weldment, where σ_z stress in longitudinal direction σ_x is the stress in transverse direction and σ_y is the stress in the thickness direction. When comparing SS400 with STS304, only in base metal except for weld, the higher residual stress σ_x is generated in STS304, but the higher residual stress, σ_y is generated in SS400.

2) Welding residual stresses of numerical analysis on dissimilar SS400-STS304 steel weldment are identical in the distributional aspects of those with measurement and a minute increase occurs.

3) When comparing the obtained analysis results, with and without welding residual stress for dissimilar SS400-STS304 steel weldment under superimposed external load (tension load), the difference has been clearly noticed. Especially, the longitudinal tensile residual stress σ_z is increased significantly to a higher value.

4) Mechanical tests and metallurgical analysis was carried out to ensure the weld integrity and the results were found satisfactory without weld defects.

ACKNOWLEDGEMENT

This work was supported by the Korea Research Foundation Grant funded by the Korean Government (MOEHRD, Basic Research Promotion Fund) (KRF-2006-531-D00054).

REFERENCES

1. H.S. Bang : Study on the mechanical behavior of welded part in thick plate - three-dimensional thermal elasto-plastic analysis based on finite element method, Journal of the Korean Welding Society, **10-4** (1992), 37~43 (in Korean)
2. H.S. Bang, H.S. Bang, S.M. Joo: Numerical simulation of Al-SPCC weldment, Key Engineering Materials, Oct., 2006, 1738-1744 (in English)
3. Rajesh S.R, H.S. Bang, S.M. Joo, I.S. Kim: Study on the effect of residual stress on the externally loaded welded structure, Journal of the Korean Welding Society, **Vol 43** (2004), 58~60 (in Korean)
4. Koichi Masubuchi: Analysis of Welded Structures, Pergamon Press
5. Material properties database, copyright © 2003, JAHM Sofware, Inc
6. Y.Ueda, Y.C.Kim, H.S Bang: Mechanical characteristics of repair weld in thick plates, Transaction of JWRI, 15-2, 1987 (in Japanese)